Electron transfer processes between sputtered O atoms and Ag(110):O(n × 1) reconstructed surfaces

2008 J. Phys.: Condens. Matter 20 355008

(http://iopscience.iop.org/0953-8984/20/35/355008)

J. Phys.: Condens. Matter **20** (2008) 355008 (7pp) doi:10.1088/0953-8984/20/35/355008

Electron transfer processes between sputtered O atoms and Ag(110):O($n \times 1$) reconstructed surfaces

L Guillemot[1,2,4], Y Bandurin[3], K Bobrov[1,2] and V A Esaulov[1,2]

[1] CNRS, UMR 8625, Laboratoire des Collisions Atomiques et Moléculaires, LCAM, Bâtiment 351, UPS-11, F-91405 Orsay, France
[2] LCAM, Université Paris-Sud, F-91405 Orsay, France
[3] Uzhgorod Centre, Kiev National Trade-Economic University, Korytnjanska, 4. 88020 Uzhgorod, Ukraine

E-mail: laurent.guillemot@u-psud.fr

Received 2 May 2008, in final form 17 July 2008
Published 13 August 2008
Online at stacks.iop.org/JPhysCM/20/355008

Abstract

We present results of a study of sputtered oxygen atom outgoing trajectory dependence of the electron transfers with oxidized Ag(110) surfaces reconstructed in different ($n \times 1$) added row structures. With a charge state resolved time-of-flight–direct recoil spectroscopy investigation using 4 keV Ar^+ incident ions, we determine relative yields of sputtered O and Ag atoms as well as the fraction of sputtered O^- ions, for different incident polar and azimuthal angles. The relative yields of sputtered O atoms are satisfactorily reproduced by a classical dynamics simulation. No sputtered Ag^- ions were detected. A qualitative discussion of the features of the oxygen negative ion fractions suggests that its description needs, in general, to take into account both capture and loss of electrons as the oxygen atom leaves the surface. The experimental data also suggest that one needs to correctly describe the corrugation of the surface and that the electron loss rates should be site-specific.

1. Introduction

Many chemical reactions of interest for industrial or technological use actually take place at the surface of metals. The presence of impurities at the surface can strongly influence those reactions. Thus alkaline species can efficiently promote the catalytic activity of transition metals, and on the other hand electronegative adsorbates such as O, S or halogens are usually known to poison the reactivity of a surface. In the case of the silver surface it is well known that oxygen and chlorine pre-adsorption plays a key role in the epoxidation of ethylene. The ability of the oxidized surface to exchange electrons with O atoms is thus of great interest.

The adsorption of oxygen on silver surfaces has been, in the last few decades, the subject of numerous experimental and theoretical studies [1–6]. It is now well established [1, 7] that above 190 K O_2 dissociates to adsorb on Ag(110) and induces a well-ordered reconstruction leading to the formation of added rows of alternating O and Ag atoms along the [001] direction, with an $n \times 1$ periodicity along the $[1\bar{1}0]$ direction, n depending and decreasing with the oxygen coverage (figure 1). It should be noted that the oxygen covered surface, even at saturation coverage in the O(2×1) reconstruction, keeps a metallic character with essentially covalent bindings between O and Ag atoms.

This system seems well suited to further our investigations [8–10] of the adsorbate-induced modifications of the electron transfer rates on metal surfaces and especially put some emphasis on the role of adsorbate-related local electronic modifications of the metal surface in a system where adsorbate positions and relative distances are known and can be varied in a controlled manner with oxygen dose.

Charge state resolved–direct recoil spectroscopy (CSR-DRS) was previously used to study the Ni(100)-$c(2 \times 2)$O system [11, 12]. It differs from the present one in that no complex reconstruction is induced, the oxygen atoms simply sitting 0.9 Å above the last metal atom layer, in the fourfold hollow sites. This study revealed strong azimuth and exit angle dependence of the sputtered O^- fractions. The main

[4] Author to whom any correspondence should be addressed.

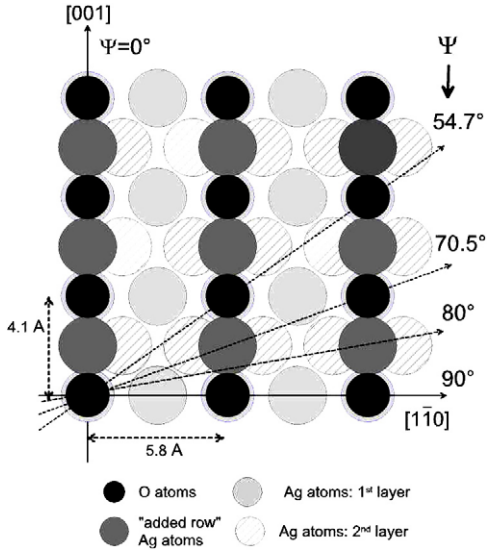

Figure 1. Model of the Ag(110) + O(2 × 1) reconstructed surface.

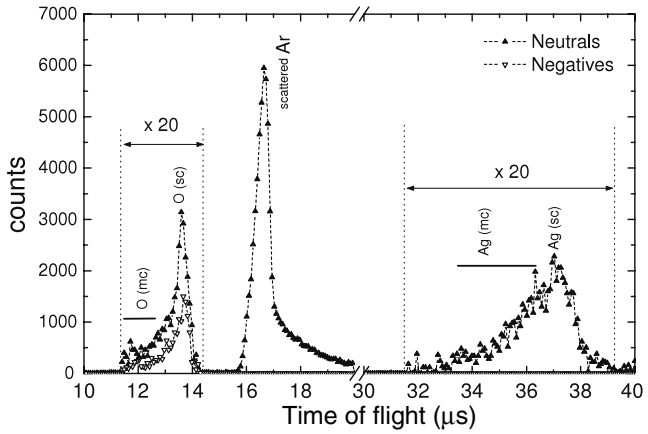

Figure 2. Typical TOF spectra of scattered or sputtered neutral and negative particles under a 4 keV Ar^+ ion bombardment of a Ag(110) + O(2 × 1) surface with $\alpha = 8°$ and $\Psi = 70°$. Total scattering angle $\theta = 38°$. The main peaks are assigned to scattered Ar, sputtered oxygen and silver, showing contributions from single (sc) and multiple (mc) collisions. The vertical scale is magnified by a factor of 20 in the O and Ag peak regions.

features of the experimental results were shown to be due to the corrugation of the surface electrostatic potential induced by the adsorbate negative charge state related dipoles. This corrugation causes an upward shift of the O^- affinity level on top of the adsorbate sites. This shift was found to be responsible for larger electron loss to the metal valence band and explain the lower O^- fractions found in the oxygen-rich exit directions for intermediate exit angles.

2. Experimental details

Our experiments were performed on a set-up described in detail elsewhere [13]. The set-up allows us to perform time-of-flight (TOF) spectroscopy, Auger electron spectroscopy (AES) and low energy electron spectroscopy (LEES). Ar^+ ions are produced in a discharge source, mass-selected and steered into the main UHV chamber. The pressure in the UHV chamber is typically 2×10^{-10} Torr. The commercial Ag(110) sample was polished to 0.05 μm and oriented to within 0.5°. *In situ* preparation consisted in repeated cycles of Ar^+ grazing incidence sputtering and annealing. Surface cleanliness was ascertained by AES and by performing a TOF analysis of scattered and recoiled particles for Ar^+ incident ion scattering. A clean metal surface condition was considered to be one in which direct recoiled peaks of impurities such as H, C and O were not visible in the TOF spectra [13].

The time-of-flight–direct recoil spectroscopy is performed using a chopped beam of 4 keV Ar^+ ions using voltage pulses of 30 V amplitude and 100 ns time width, scanning the beam across a 2 mm wide slit. The scattered or sputtered particles are detected at a fixed scattering angle of 38° at the end of a 2.24 m long flight path, onto a position-sensitive 30 mm diameter channel plate detector, equipped with three discrete anodes. A deflector plate assembly set before the channel plates allows splitting the incoming ions and neutrals, which are detected simultaneously by each anode. The oxygen adsorption was done by letting in a controlled pressure of oxygen into the chamber in a range of 10^{-6}–10^{-4} mbar, on a surface previously heated to 200 °C, for times of typically 10 to 20 min (final temperature was typically 100 °C). One can simultaneously measure time-of-flight spectra for neutral particles as well as positive or negative ions. As this study deals with the formation of O^- ions, we will focus on the neutral particle and negative ion TOF spectra. Only minute amounts of positive ions were detected in the conditions of this set of experiments.

The oxygen doses required to get the different ($n \times 1$) reconstructed structures were carefully calibrated according to the work function change of the surface [1, 10]. This work function change with oxygen dose was monitored by measuring the shift of the threshold of the secondary electron energy distribution emitted under He^+ ion bombardment.

3. Results and discussion

Measurements of time-of-flight spectra were performed for various Ar ion incident angles (α) and for various azimuthal (Ψ) orientations of the target. Since the total scattering angle in this experiment is fixed at 38°, a variation in α leads to a variation in the exit angle β of the exiting scattered or sputtered particles.

A typical TOF spectrum of scattered and sputtered particles is shown in figure 2. In the neutral TOF spectra different peaks can be assigned to either scattered Ar or sputtered O and Ag atoms. In the negative ion spectra only structures related to sputtered O^- ions are visible and no Ag^- ions were detected (figure 2).

In the conditions of our experiment, for the simplest cases of single-collision processes, the energies of the detected particles are 3410 eV for scattered Ar, 2030 eV for sputtered O and 1960 eV for sputtered Ag.

Intensities of the different peaks $I(\mathrm{Ar})$, $I(\mathrm{O}^0)$, $I(\mathrm{O}^-)$ and $I(\mathrm{Ag})$ can be measured. We shall also split the peak of sputtered O into two contributions: $I(\mathrm{O_{sc}})$ for the

thin, well-defined peak at 13.5 μs corresponding to single collisions (sc) and $I(O_{mc})$ for the rest of it, at smaller times corresponding to double and multiple collisions (mc). The ratio $I(O_{sc})/(I(O_{sc}) + I(O_{mc}))$ is of interest to get some idea whether the O atoms were mainly sputtered by hard head-on collisions or a combination of several collisions.

The TOF spectra were used to extract negative ion fractions (Φ_O^-). The Φ_O^- fraction was determined as a function of the exit angle β and the azimuthal one Ψ, i.e.

$$\Phi_O^-(\beta, \Psi) = \frac{I_O^-(\beta, \Psi)}{I_O^-(\beta, \Psi) + I_O(\beta, \Psi)}.$$

In the following we shall present and discuss the characteristics of measured atom and anion yields and negative ion fractions. In order to get some insight into the measured O yields, we performed some classical dynamic simulations using the SNOOK code from the Kalypso package [14] with the following characteristics: the target was made of a slab of 9 × 9 atoms in the surface plane and four layers on top of which are placed the added rows at a 0.145 nm vertical distance corresponding to an unreconstructed first layer. ZBL interaction potentials [15] were used for Ar/Ag and Ar/O as well as between surface atoms. Trajectory calculations were done for a set of incident polar and azimuth angles and the sputtered O particles were geometrically selected to simulate our detection system. For $\Psi = 90°$ (perpendicular to the added rows) preliminary calculations showed that the O yield was due almost exclusively to trajectories passing above the lines of O atoms. Several thousand trajectories scattered along the [001] direction on top of the O atoms were sufficient to get the full exit angle dependence. For the incident azimuthal angle dependence, such simplification was not possible, and a much larger number—400 000 trajectories—spread over the whole Ag(110) + O(2 × 1) unitary mesh was required for each angle to provide sufficient statistics.

3.1. O yields

Let us turn first to basic information that one readily gets out of our TOF-DRS data, that is the O yield dependence with either polar α or azimuth Ψ incident angles. One is interested here in the total O yield, irrespective of the charge state of the particles.

For the Ag(110) + O(2 × 1) surface, one can see in figure 3(a) the O yield dependence with the incidence angle α, at a particular $\Psi = 90°$ azimuth, corresponding to a direction of the incoming Ar^+ ions perpendicular to the Ag–O–Ag chains. Below $\alpha = 5°$, there are virtually no O atoms detected. The yield then increases between 5° and 10°, levelling off around $\alpha = 11°$ and then decreasing smoothly down to nearly zero at 30°. This behaviour is consistent with a situation where the O atoms in the added rows are shadowed by the O atoms in the row next to it. This picture is further confirmed by the evolution of the $I(O_{sc})/I(O^0)$ ratio (not shown) which rises steeply from 35% at $\alpha = 10°$ to nearly 70% at $\alpha = 20°$. The α dependence in this case is satisfactorily reproduced by the simulation even though the experimental distribution is wider. This could be due to the fact that all the simulations have been made at a 0 K surface temperature. As a matter of fact the very

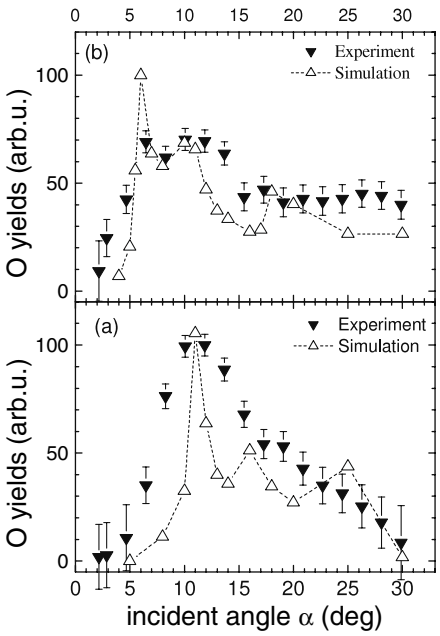

Figure 3. Total sputtered O yields (experiment and simulation) as a function of the incident polar angle α for a $\Psi = 90°$ incident azimuth angle on (a) Ag(110) + O(2 × 1) and (b) Ag(110) + O(4 × 1), reconstructed surfaces.

steep threshold of the simulated O yield between $\alpha = 8°$ and 10°, exactly matches the value expected from the shadowing by the added rows, 5.8 Å apart in the (2 × 1) reconstruction with frozen atoms. The fact that clear non zero yields are measured for α angles down to 5° could be due to an incomplete (2 × 1) reconstruction, some small parts of the surface having only (3 × 1) or (4 × 1) added row structures.

In the case of Ag(110) + O(4 × 1), figure 3(b) shows a shift of the threshold of the O yield distributions to smaller α. Accordingly the $I(O_{sc})/I(O^0)$ ratio shows a strong increase from 25% to 50% for the lower range of $\alpha = 2°$–9°. Here again a reasonable agreement is found between experiment and simulation. The maximum at $\alpha = 6°$, very sharp in the simulated distribution, is present but only faintly visible in the experimental data, and its clear dominance with respect to a secondary maximum at $\alpha = 10°$ is not seen in the experiment. This difference in the relative importance of the two maxima could be due to a partial presence of (2 × 1) reconstructed patches, giving a maximum contribution of the O yield right at the α value where the secondary maximum of the rest of the (4 × 1) surface is located.

One now turns to the Ψ dependence of the O yield, on the Ag(110) + O(2×1) surface. It is noteworthy that the O yield is vanishingly small in the $\Psi < 20°$ range when the incident ion beam is close enough to the [001] direction that each O atom is shadowed by the Ag atom next to it in the same added row. Above this 20° threshold, one gets some O yield. In general we observe that oxygen sputtering is strongest for the incident ion beam directions at 35° to the added rows, where oxygen is more 'visible' to the incident beam. We will now focus on a region where the most remarkable features in the yield (figure 4) are located within ±25° around $\Psi = 90°$ azimuth

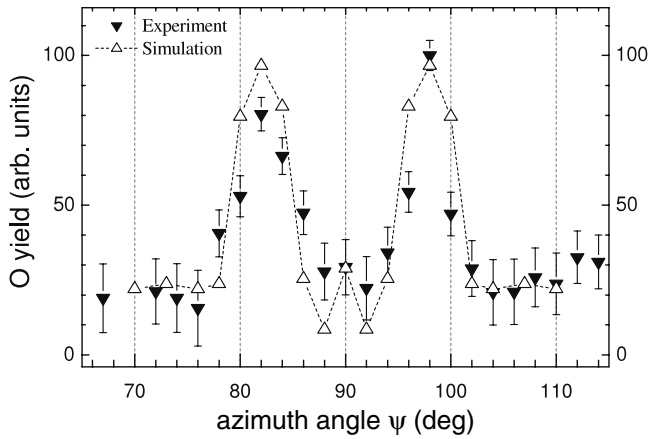

Figure 4. Total sputtered O yields (experiment and simulation) as a function of the azimuth angle Ψ, for $\alpha = 8°$ ($\beta = 30°$) incident polar angle on a Ag(110) + O(2 × 1), reconstructed surface.

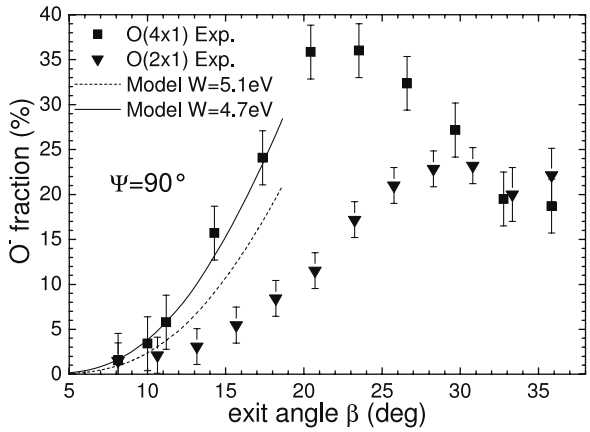

Figure 5. O^- ion fractions as a function of β, the exit angle with respect to the surface, for an incident azimuth angle $\Psi = 90°$, for O(2 × 1) and O(4 × 1) surface reconstructions.

which corresponds to incoming Ar^+ ions perpendicular to the Ag–O–Ag chains. The experimental results show clear maxima at ±8° on each side of the $\Psi = 90°$ direction, where the yield is rather small. The simulation accounts very well for the position of the experimental findings even though the width of the simulated features are somewhat larger than the experimental ones. This could be related to the fact that we had to use a simulated detector angular aperture larger than the actual experimental one, in order to reach reasonable statistics in our simulation results.

Thus the general characteristics of the sputtered oxygen can be well accounted for in this simulation.

3.2. Negative ion fractions

Before considering oxygen, a first interesting experimental observation is that no sputtered Ag^- ions were detected either on the oxygen-covered surfaces or on the clean Ag(110) surface. In the conditions of our experiments and with our background level in the negative ion spectra we estimate the Ag^- ion fraction to have an upper limit of 1%.

Figure 5 displays the Φ_O^- fractions measured as a function of the exit angle β, for a given azimuthal angle $\Psi = 90°$ and for the two oxygen coverages corresponding to the O(2 × 1) and O(4 × 1) surface reconstructions. In both cases, a strong variation of the O^- fraction is measured with some threshold exit angles below which no appreciable amount of O^- ions is detected, followed by a strong increase up to a maximum value. In the case of the O(4 × 1) reconstruction, a slight decrease is then observed. If the threshold values for both surfaces seem to be close to 7°, the increase is much sharper in the case of the O(4 × 1) surface, leading to a maximum value of 35% at 22°, notably larger than the 22% reached at 30° on the O(2 × 1) surface. It should be noticed that the Φ_O^- (β) behaviour is similar, whatever the Ψ angle investigated.

In the case of the Ψ dependence figures 6(a) and (b) show that for $\beta = 30°$ the O^- fraction is found to be weakly dependent on the incident azimuth for both coverages. At smaller β value, on the other hand, a broad maximum appears around the $[1\bar{1}0]$ direction with a local minimum right at the $\Psi = 90°$ azimuth, clearly observable for the (2 × 1) surface reconstruction. In this case the local maxima are centred at about ±7° on each side of the local minimum, close to the position of the O yield maximum, but are wider. The overall width of this hump appears wider for the (2 × 1) case. We emphasize that the appearance of these local maxima in Φ_O^- (Ψ) at ±7° from the $[1\bar{1}0]$ axis cannot be related to the maxima in the total O yield at ±8°.

The first point that can be addressed is the magnitude of the O^- fractions that we get in this (CSR-DRS) experiment. A reference mark can be found in a scattering experiment [16] where the production of O^- ions was monitored as a function of the exit angle of the particles after scattering on different metal surfaces among which was poly-crystalline silver. Interpolating from the 4 and 1 keV incident energy results, one can assess a typical O^- fraction of 10% for a 2 keV energy and a 30° exit angle of interest here. One should notice that in these experiments, it is also found that the scattered O^- fraction is the same, whatever the charge state (O^- or O^0) of the incident particles. This gives evidence that the final charge fraction measured results from a balance between capture and loss processes in the outgoing trajectory only. This situation is comparable to the present one, where by definition the sputtered O atoms/ions only experience processes in the outgoing trajectory.

It is well known that oxygen adsorption on a silver surface increases its work function and specifically there is a 0.8 eV increase at maximum coverage in the case of Ag(110) + O(2 × 1), with respect to the clean Ag(110) surface [1, 10]. A work function increase is known to lower the negative ion production, because the electron losses, energetically possible at smaller atom–surface distance, become more efficient. On the other hand, we have shown on several examples [8–10] that changes in the production of negative ions on oxygen-covered metal surfaces cannot be simply understood in terms of the change of work function which is a macroscopic averaged property. Not to be disregarded are the effects of changes in the local electronic structure in the vicinity of the adsorbate,

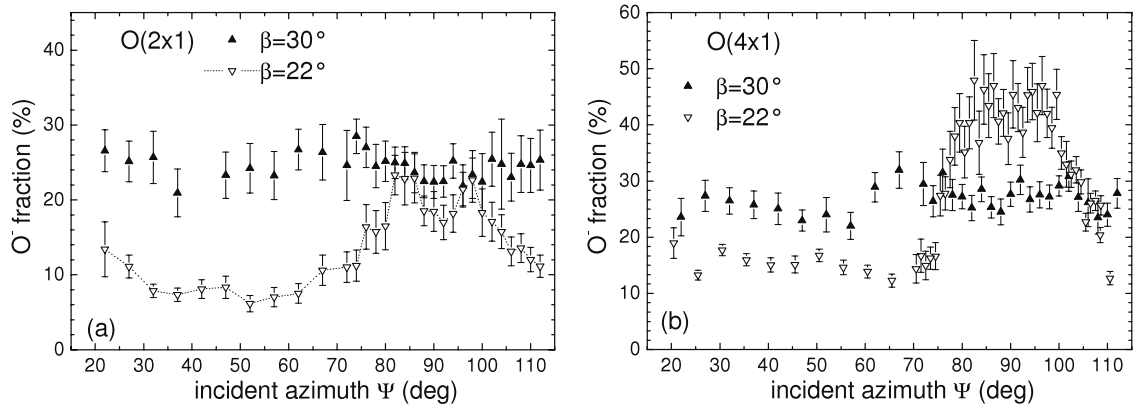

Figure 6. O^- ion fractions as a function of incident azimuth angle Ψ at exit angles $\beta = 30°$ and 22° for (a) the O(2 × 1) and (b) the O(4 × 1), reconstruction structures.

that can drastically change the capture/loss rates. In this particular case of an oxygen-covered Ag(110) surface, the strong work function increase should lead to a strong decrease in O^- production. On the other hand, strong local electronic effects, if any, could attenuate this decrease by reducing the electron losses to the surface. In practice we see that the O^- fraction measured for the 30° exit angle in our (CSR-DRS) on the Ag(110) + O(2 × 1), instead of being smaller than the 10% on the clean silver surface, is more than twice as large.

A proper discussion of the behaviour of the oxygen ion fractions should rely on the knowledge of the site-specific interaction widths, which are not known. In particular the electron capture and loss rates are most probably different above the Ag or O atoms of the added rows and also the areas of the Ag surface without oxygen. Here we shall point out some factors which could be responsible for the increased negative ion production and for the type of azimuthal angular dependence we observe.

The first one is related to a peculiarity of the electronic structure of the Ag(110) surface, which is the existence of a surface state (SS) dispersing around the Y direction of the surface Brillouin zone (SBZ) with a minimum energy of 1.65 eV above the Fermi level. This feature has been first shown by an inverse photoemission study two decades ago [17]. In the case of scattering experiments, it opens a loss channel for a departing O^- ion at a distance of 3 Å from the clean Ag(110) surface. Even though this loss channel should not be dominant with respect to the 3D continuum available close to the Γ point, it has been shown that this SS is efficiently quenched by the presence of even a very small dose of oxygen [17]. That means that on the oxygen-covered silver surface this electron loss channel is suppressed. This should favour a higher O^- fraction measured in this CR-DRS experiments.

A second point could be related to the initial vertical position of the O atoms in the added rows. If one takes the image plane of the first atomic layer of the clean Ag(110) surface as the zero distance reference, it should be remembered that an O^- ion, leaving the surface, starts to lose its electron when its affinity level crosses above the Fermi level of the Ag(110) surface at some 1.35 Å from the surface. In the case of an oxygen-covered silver surface with a work function 0.8 eV larger ($\phi = 5.1$ eV), this distance goes down to 1.0 Å. Actually, the sputtered O atoms are sputtered off the added rows and are then sitting in an initial position at a distance of 1.45 Å considering nonreconstructed first and second layers or even 1.55 Å according to a photoelectron diffraction study [18]. This means that the O ion does not experience the initial 0.5 Å distance of the exit trajectory, where the electron loss is most efficient. That could contribute to the high O^- fractions measured in our CR-DRS experiments. It should be noted, however, that in this argument we assumed that the image plane corresponds to that of the clean Ag surface and not the oxygen-covered one. However, in all cases the strong corrugation of the surface should lead to changes not observed on the 'flat' Ag(110) surface, as will be discussed below.

The behaviour of Φ_O^- against β is noteworthy. The increase of the negative ion fraction in the 10°–20° (or 30°) range fits in a simple picture of ion survival getting larger as the exit angle, i.e. the normal outgoing velocity, increases.

One can find some quantitative support of this idea in a paper by Bahrim *et al* [19] who made calculations of the fraction of negative oxygen ions sputtered from metallic surfaces for different values of the work function, calculations that were able to correctly reproduce experimental results obtained from metallic surfaces with different alkali coverages [20]. Yu originally fitted his results by the empirical formula $\Phi_O^- \approx A \times \exp(\frac{-\varepsilon(V_{\rm perp})}{W})$, where W is the surface work function and ε is a parameter which has been evaluated in [17] for a range of $V_{\rm perp}$, normal velocities of the outgoing sputtered atoms. Extrapolating the ε values for velocities up to 60 km s^{-1}, we calculated the O^- fraction for a corresponding exit angle range up to 18°, in our experiment. The results are shown in figure 5, taking $W = 5.1$ and 4.7 eV for the O(2 × 1) and O(4 × 1) surfaces, respectively.

We determined a pre-exponential factor $A = 10.0$ to reproduce the experimental O^- fraction value for the O(4 × 1) surface at the smallest measured exit angle. The exit angle dependence for the O(4 × 1) surface is satisfactorily reproduced, giving nice evidence that, in this exit angle range, the negative ion survival model holds. Nevertheless the results

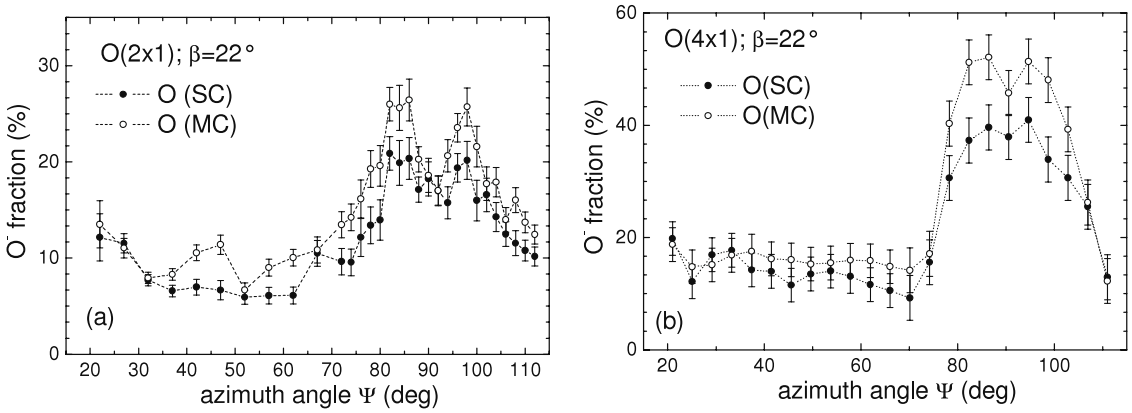

Figure 7. O^- ion fractions of the sputtered oxygen resulting from single (SC) or multiple (MC) collisions as a function of incident azimuth angle Ψ at exit angles $\beta = 22°$ for (a) the O(2 × 1) and (b) the O(4 × 1) reconstruction structures.

for the O(2 × 1) surface overestimate the experimental values which increase to a lesser extent with β.

Thus the predictions of the model, which basically treats the two surfaces on an equal footing, taking into account only the difference in work function, shows that if qualitatively the behaviour is the one expected, quantitatively the difference is more pronounced in the experimental results. Structural differences should play a role here and in particular the fact that, for the same exit angle with respect to the surface on the 2 × 1 surface, the outgoing O^- meets the next added row at a closer inter-atomic distance than for the 4 × 1 surface, leading to a larger electron loss.

Furthermore the decrease of the ion fraction at larger angles for the O(4 × 1) surface (plateau observed for the O(2 × 1)) would actually suggest that one needs not only to consider survival, but also take into account an initial electron capture process leading to the negative ion formation.

Let us now turn to the behaviour of Φ_O^- with respect to Ψ. For the $\beta = 30°$ case, at strong variance with the O/Ni(100) system, no strong azimuthal effects corresponding to ion trajectories passing above oxygen or above silver atoms were observed. The most striking feature is the presence of the double 'hump' in the $\Phi_O^-(\Psi)$ around the $[1\bar{1}0]$ direction for $\beta = 22°$. This effect is important in terms of the Φ_O^- values which are 3 to 4 times larger at the maximum than outside of this angular range.

In the case of the O(2 × 1) surface, the clearly pronounced double peak structure closely corresponds to the case of the O^- ions flying between the Ag and O atoms of the next added row. This is less pronounced for the O(4 × 1) surface. Both maxima sit (7±0.5)° away from the local minimum in the O(2 × 1) case and (5 ± 1)° in the O(4 × 1) case. The exact middle of the Ag and O atoms of the next row, for the O(2 × 1) surface, should actually be 10.2°. A plausible explanation for the local maxima is that for the same exit angle the actual distance between the outgoing oxygen and the next added row surface atom is larger in between these atoms than on top. In this case, assuming a 'corrugated' interaction width, we should observe less loss and a higher negative ion fraction. In this context a very interesting point is the appearance of the maximum at 7° rather than at 10°, which may imply some difference in interaction with the O and Ag atoms in the added row. The fact that for the 30° exit angle such a strong increase is not observed at these angles could be due to the larger oxygen–surface distance, where the corrugation is not felt as strongly. It is interesting to note that we have observed similar features in fluorine anion fractions in F scattering on this AgO surface [21].

Finally we examine the finer difference in the sputtered O intensities in the two already mentioned components: O atoms sputtered from single collisions (SC) or from multiple collisions (MC). The latter ones are identified in the TOF spectra as more energetic O atoms. This contribution extends, on a rather large time range, the mean value corresponding to a 35% larger energy (2740 eV) than the one for the SC case (2030 eV). The negative ion fraction is shown in figures 7(a) and (b). It is found that the $\Phi_O^-(\Psi)$ values of the MC component are typically 30% higher than the ones for the SC component. This result can be readily understood in the simplest scenario, negative ions being ejected from the surface and the measured negative ion fraction reflecting the ion survival, which is more important for more energetic ions, getting away from the surface at higher velocity.

This simplest scheme does not hold in all angular configurations investigated. Thus for the 30° exit angle, one measures no significant differences in the $\Phi_O^-(\Psi)$ values for the SC and MC components (not shown). Here again we may need to take into account the initial negative ion formation probability for the sputtered oxygen.

One last interesting feature of this system needs to be pointed out. Till now we only considered the interaction of oxygen with its neighbouring Ag and O atoms. However, in the direct recoiling process we actually deal with an oxygen atom receding from the surface, while at the same time the Ar atom is scattering into the surface below it. In a way, we may have a situation where, in an initial part of the receding trajectory, the Ar 'screens' off the Ag surface from the departing oxygen.

4. Conclusion

We have presented results of a study of sputtering of oxygen atoms and anions from a reconstructed oxygen-covered Ag surface. The general characteristics of the total

sputtered oxygen yield as a function of exit angle and surface azimuthal orientation could be adequately described using the classical scattering dynamics code SNOOK. Our results reveal interesting exit and azimuth angle dependence. A qualitative discussion of the features of the negative ion fractions suggests that its description needs to take into account both capture and loss of electrons as the oxygen atom leaves the surface. The experimental data also suggest that one needs to correctly describe the corrugation of the surface and that the electron loss rates should be site-specific. An interesting extension of this work would involve a study of the characteristics of O^- production by scattering of O atoms on the $Ag(110) + O(n \times 1)$ surfaces. We hope these results will stimulate a theoretical study of this system.

References

[1] Canepa M, Cantini P, Fossa F, Mattera L and Terreni S 1993 *Phys. Rev.* B **47** 15823

[2] Canepa M, Cantini P, Mattera L, Terreni S and Valdenazzi F 1992 *Phys. Scr.* **41** 226

[3] Canepa M, Salvietti M, Traverso M and Mattera L 1995 *Surf. Sci.* **331** 183

[4] Hashizume T, Taniguchi M, Motai K, Lu H, Tanaka K and Sakurai T 1991 *Japan. J. Appl. Phys.* **30** 1529

[5] Sesselman W, Woratschek B, Kuppers J, Ertl G and Haberland H 1987 *Phys. Rev.* B **35** 1547

[6] Vatuone L, Rocca M, Restelli P, Pupo M, Boragno C and Valbusa U 1994 *Phys. Rev.* B **49** 5113

[7] Guillemot L and Bobrov K 2007 *Surf. Sci.* **601** 871

[8] Maazouz M, Guillemot L, Lacombe S and Esaulov V 1996 *Phys. Rev. Lett.* **77** 4265

[9] Ustaze S, Guillemot L, Verruchi R and Esaulov V 1998 *Surf. Sci.* **397** 361

[10] Ustaze S, Lacombe S, Guillemot L, Esaulov V and Canepa M 1998 *Surf. Sci.* **414** L938

[11] Hsu C C, Bousetta A, Rabalais J W and Nordlander P 1993 *Phys. Rev.* B **47** 2369

[12] Hsu C C, Bu H, Bousetta A and Rabalais J W 1992 *Phys. Rev. Lett.* **69** 188

[13] Esaulov V, Guillemot L, Grizzi O, Huels M, Lacombe S and Tuan V N 1996 *Rev. Sci. Instrum.* **67** 135

[14] Karolewski M 2004 *Nucl. Instrum. Methods* B **230** 402

[15] Ziegler J F, Biersack J P and Littmark U 1985 *The Stopping and Ranges of Ions in Solids* vol 1 (Oxford: Pergamon)

[16] Maazouz M, Guillemot L, Schlathölter T, Ustaze S and Esaulov V 1997 *Nucl. Instrum. Methods* B **125** 283

[17] Reihl B and Schlittler R R 1984 *Phys. Rev. Lett.* **52** 1826

[18] Pascal M, Lamont C L A, Baumgärtel P, Terborg R, Hoeft J T, Schaff O, Polcik M, Bradshaw A M, Toomes R L and Woodruff D P 2000 *Surf. Sci.* **464** 83

[19] Bahrim B, Teillet-Billy D and Gauyacq J P 1994 *Surf. Sci.* **316** 189

[20] Yu M L 1981 *Phys. Rev. Lett.* **47** 1325

[21] Canario A R, Guillemot L, Valdes J, Vargas P and Esaulov V A 2008 *Phys. Rev.* A at press